Detection and suppression of epileptiform seizures via model-free control and derivatives in a noisy environment

Cédric Join, D. Blair Jovellar, Emmanuel Delaleau, Michel Fliess

Detection and suppression of epileptiform seizures via model-free control and derivatives in a noisy environment

Cédric Join[1,6], D. Blair Jovellar[2,3], Emmanuel Delaleau[4] and Michel Fliess[5,6]

***Abstract*— Recent advances in control theory yield closed-loop neurostimulations for suppressing epileptiform seizures. These advances are illustrated by computer experiments which are easy to implement and to tune. The feedback synthesis is provided by an intelligent proportional-derivative (iPD) regulator associated to model-free control. This approach has already been successfully exploited in many concrete situations in engineering, since no precise computational modeling is needed. iPDs permit tracking a large variety of signals including high-amplitude epileptic activity. Those unpredictable pathological brain oscillations should be detected in order to avoid continuous stimulation, which might induce detrimental side effects. This is achieved by introducing a data mining method based on the maxima of the recorded signals. The real-time derivative estimation in a particularly noisy epileptiform environment is made possible due to a newly developed algebraic differentiator. The virtual patient is the Wendling model, i.e., a set of ordinary differential equations adapted from the Jansen-Rit neural mass model in order to generate epileptiform activity via appropriate values of excitation- and inhibition-related parameters. Several simulations, which lead to a large variety of possible scenarios, are discussed. They show the robustness of our control synthesis with respect to different virtual patients and external disturbances.**

***Index Terms*— Epileptiform seizures, neurostimulation, seizure detection, seizure suppression, model-free control, intelligent proportional-derivative controller, noise removal, algebraic differentiator, data mining.**

I. Introduction

The complexity of brain explains why the *closed-loop*, or *feedback*, setting, which is a key concept in control theory, is so underdeveloped in computational neuroscience as analyzed in several recent publications (see, e.g., [1], [2], [3], [4], [5]), in spite of some preliminary attempts (see, e.g., [6]). This is confirmed [7] by the secondary role of brain research in *systems biology*, a discipline that focuses on the connections between biology and control systems (see, e.g., [8], [9]).

This communication reports some preliminary computer experiments on *epilepsy*, an important neurological disorder, also known as a *seizure disorder* [10]:

1) A closed-loop seizure suppression is proposed. It is based on an *intelligent* regulator derived from *model-free* control (MFC) [11], [12]. This setting has already led to many concrete applications (see, e.g., references in [11], [12]). Let us emphasize here a most recent comparison [13] with other popular types of control synthesis in some specific questions arising in intelligent transportation systems, where the superiority of MFC is asserted. See below some of its main features:
   - MFC does not necessitate any mathematical modeling, and therefore neither delicate parameter identification procedures.
   - It is much easier to tune than proportional-integral-derivative (PID) controllers which are the most popular industrial feedback loops (see, e.g., [14]).
   - It has already been successfully illustrated in biomedicine and bioengineering [15], [16], [17], [18], [19].

   Following [12], the use of an *intelligent proportional-derivative* controller, or *iPD*, seems more adapted to regulate, via electric stimulations, a large variety of high-amplitude epileptic activity.
2) Those aberrant burst events recur unpredictability and often are separated by long interictal time lapses. A continuous stimulation like above might therefore induce detrimental side effects [20]. A real-time seizure detection is thus necessary for triggering the above feedback. Frequency-domain techniques are today a crucial ingredient in most publications on this subject (see, e.g., [21], [22], [23], [24], [25], and references therein). We follow here another quite recent route using algebraic manipulations in the time-domain (see [26], [27], [28], for the theoretical background and the presentation of successful applications), and more specifically, here, via a new data mining viewpoint [29] where the maxima of the recorded signal are determined. Let us summarize this approach:
   - Maxima in a seizure are large and close to each other.
   - Using derivatives for seizure detection, which involves a noisy environment, is a known challenge in engineering.
   - Our *algebraic differentiator*, which is borrowed from [30] (see, also, [31]), does not necessitate any probabilistic and/or statistical assumption on the noise corruption.
3) The *virtual* patient, i.e., the epileptiform signal, is

[1]CRAN (CNRS, UMR 7039)), Université de Lorraine, BP 239, 54506 Vandœuvre-lès-Nancy, France. *@: cedric.join@univ-lorraine.fr*

[2]Department of Neurology & Stroke, University of Tübingen, Tübingen, Germany. *@: desiree-blair.jovellar@uni-tuebingen.de*

[3]Hertie-Institute for Clinical Brain Research, University of Tübingen, Tübingen, Germany.

[4] ENI Brest, IRDL (CNRS, UMR 6027), 29200 Brest, France. *@: delaleau@enib.fr*

[5] LIX (CNRS, UMR 7161), École polytechnique, 91128 Palaiseau, France. *@: Michel.Fliess@polytechnique.edu, michel.fliess@swissknife.tech*

[6] AL.I.E.N., 7 rue Maurice Barrès, 54330 Vézelise, France. *@: {cedric.join, michel.fliess}@alien-sas.com*

provided by Wendling's neural mass model [32]. This computational model, which is now recognized as an efficient approach to get insights into this disease, is deduced from the well-known Jansen-Rit set of ordinary differential equations [33] (see also [34], [35]). The stimulators location mimics [36], [37]. Modifying the many parameters of Wendling's model makes it easy to verify the inherent robustness of our model-free control.

Our paper is organized as follows. After a short presentation in Sect. II of Wendling's model where some stimulators are added, Sect. III summarizes the derivatives estimation in a noisy environment and proposes a seizure detection algorithm, which is illustrated by computer experiments. After a review of some basic aspects of model-free control, Sect. IV is discussing several scenarios on seizure suppression. See Sect. V for short concluding remarks.

II. Model

The following modification of Wendling's model [32], which is due to [36], [37], is obtained by adding stimulation (see [38] for a slightly different choice):

$$\begin{cases} \ddot{y}_0 = Aa\mathfrak{S}(u+y_1-y_2-y_3) - 2a\dot{y}_0 - a^2 y_0 \\ \ddot{y}_1 = Aa\,(p + C_2\mathfrak{S}(u+C_1 y_0)) - 2a\dot{y}_1 - a^2 y_1 \\ \ddot{y}_2 = BbC_4\mathfrak{S}(u+C_3 y_0) - 2b\dot{y}_2 - b^2 y_2 \\ \ddot{y}_3 = GgC_7\mathfrak{S}(u+C_5 y_0 - y_4) - 2g\dot{y}_3 - g^2 y_3 \\ \ddot{y}_4 = BbC_6\mathfrak{S}(u+C_3 y_0) - 2b\dot{y}_4 - b^2 y_4 \end{cases} \tag{1}$$

where

- $A, a, B, b, G, g, C_1, \ldots, C_7$ are positive constants;
- A, B and G represent the amplitude of average excitatory (EPSP), slow and fast inhibitory (IPSP) postsynaptic potentials, respectively.
- The variables y_0, y_1, y_2, y_3, y_4 represent the postsynaptic potentials of pyramidal cells, excitatory feedback, and both slow and fast inhibitory interneurons, respectively.
- $p(t)$ is an external perturbation corresponding to excitatory inputs from neighboring areas. There are various representations in the existing literature: white Gaussian noise, constant value, sum of them...
- The electrical stimulation $u(t)$ is the control variable. This follows the assumption that the stimulation generates an electric field with a direct de- or hyperpolizing linear effect onto the mean membrane potential of the neuronal subsets [39].
- The sigmoid function $\mathfrak{S}(\square)$ reads

$$\begin{aligned} \mathfrak{S}(\square) &= \frac{v_{\max}}{2}\left(1 + \tanh\frac{r}{2}(\square - v_0)\right) \\ &= \frac{v_{\max}}{1+\exp(r(v_0-\square))} \end{aligned}$$

  where $v_{\max}$ is the maximum firing rate, v_0 is the average membrane potential acting as a firing threshold, $v_{\max}$ is the maximum firing rate, and $r > 0$ is a constant.

See Fig. 1 for a block diagram description of (1), where $H_a = \frac{Aa}{s^2+2as+a^2}$, $H_b = \frac{Bb}{s^2+2bs+b^2}$, $H_g = \frac{Gg}{s^2+2gs+g^2}$ are transfer functions. The summation $y_m = y_1 - y_2 - y_3$ represents the incoming firing rate to the population of pyramidal cells.

III. Seizure detection

A. Differentiation in a noisy environment

Here we will present a simplified version, borrowed from [26]. Consider the polynomial function $\mathfrak{p}_1(t) = a_0 + a_1 t$, $t \geqslant 0$, $a_0, a_1 \in \mathbb{R}$. Classic *operational calculus* (see, e.g., [40]), or *Laplace transform*, yields $P_1 = \frac{a_0}{s} + \frac{a_1}{s^2}$. Multiply both sides by s^2:

$$s^2 P_1 = a_0 s + a_1 \tag{2}$$

Deriving both sides with respect to s, which corresponds in the time domain to the multiplication by $-t$, yields a_0:

$$a_0 = s^2\frac{dP_1}{ds} + 2sP_1 \tag{3}$$

Then a_1 is given by Eqn. (2)

$$a_1 = -s^3\frac{dP_1}{ds} - s^2 P_1 \tag{4}$$

In order to get rid of the positive powers of s, which corresponds in the time domain to derivatives w.r.t. time, multiply both sides of Eqn. (3) (resp. (4)) by s^{-n}, where the integer $n > 0$ is large enough. It yields in the time domain:

$$\frac{d\mathfrak{p}_1}{dt} = a_1 = \frac{6}{T^3}\int_0^T (-T + 2\tau)\,\mathfrak{p}_1(\tau)d\tau$$

where $T > 0$ is the window size used for the estimation. The integral, which is mitigating the corrupting noise in the sense of [41], may be in practice replaced by a digital filter. The extension to polynomials of arbitrary degree is obvious and, therefore, also to truncated Taylor expansions. Details and references on the computer implementations may be found in [31], as well as references to many concrete applications.

B. Seizure detection

A seizure may be characterized by a short time lapse between two large maxima. Those maxima correspond to zero crossings of the derivative.

An academic illustration: Take the *chirp*, i.e., a frequency modulated signal, which is familiar in radar engineering (see, e.g., [42]),

$$y(t) = \sin(2\pi t^2) + 5, \qquad 0 \leqslant t \leqslant 5$$

It is corrupted by an additive white Gaussian noise (mean: 0, standard deviation: 0.1). Fig. 2 exhibits excellent results.

Fig. 3-(a) displays a signal produced by Wendling's model [32], i.e., without stimulation, i.e., $u(t) = 0$, in Eqn. (1). Its right part shows a seizure, which ought to be detected in order to avoid any stimulation when there is no crisis [20]. The derivative of the recorded signal $y_m(t)$ is reported in Fig. 3-(b). See Fig. 3-(c) for the time lapse between consecutive maxima. The choice of an adequate threshold [29] for this time lapse yields the detection of the seizure.

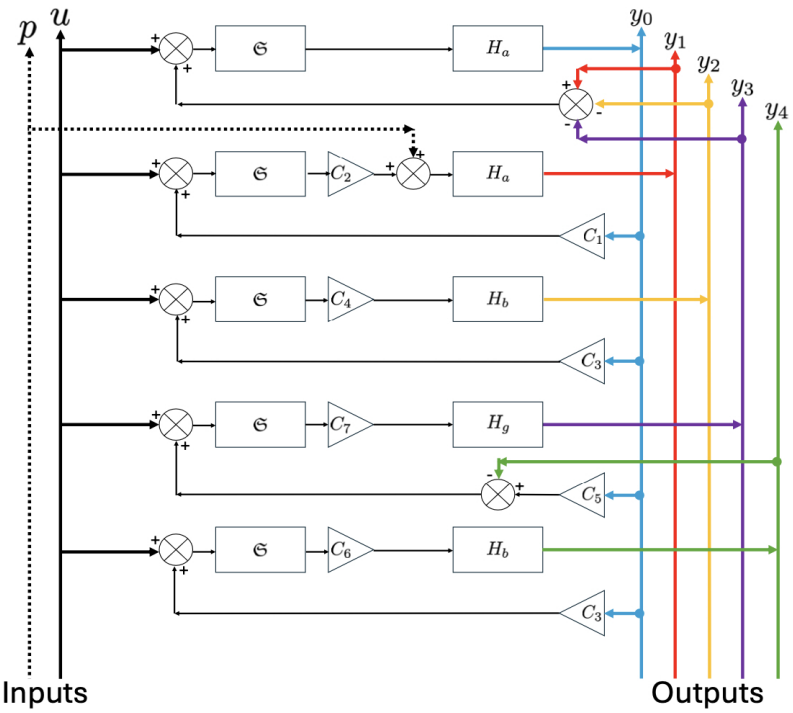

Fig. 1. Model scheme: block diagrams

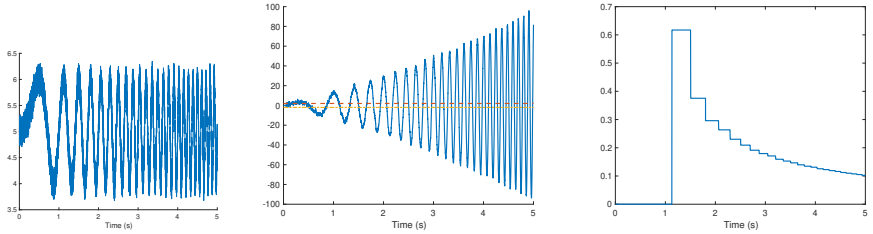

(a) y_m *(b)* Estimation of $\dot{y}_m$, zero crossing thresholds (- -) and (. -) *(c)* Time between two maxima

Fig. 2. Radar signal: Seizure detection

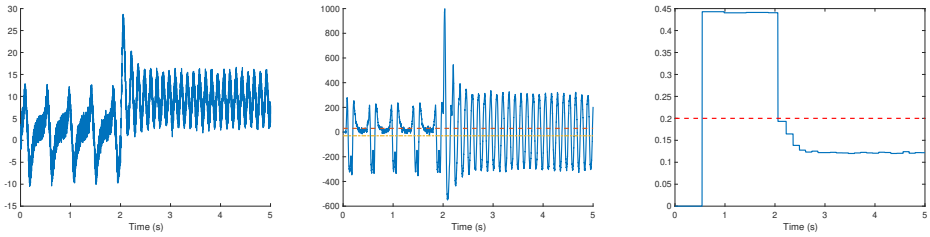

(a) y_m *(b)* Estimation of $\dot{y}_m$, zero crossing thresholds (- -) and (. -) *(c)* Time between two maxima (–) and detection threshold (- -)

Fig. 3. Epilepsy: Seizure detection

IV. Closed-loop control

A. The ultra-local model

Consider, following [12], the *ultra-local model* of order 2

$$\ddot{y}(t) = F(t) + \alpha u(t) \tag{5}$$

- $\alpha \in \mathbb{R}$, $\alpha \neq 0$, is a constant such that the three terms in Eqn. (5) are of the same magnitude. Therefore α does not need to be precisely determined.
- The *data-driven* quantity F, which subsumes not only the poorly known system structure but also any external perturbation, may be estimated via the measurements of u and y.

Introduce the *intelligent proportional-derivative* controller, or *iPD*,

$$u(t) = -\frac{F_{\text{est}}(t) - \ddot{y}^\star(t) + K_P e(t) + K_D \dot{e}(t)}{\alpha} \tag{6}$$

where

- $F_{\text{est}}(t)$ is an estimate of F (see Eqn. (7));
- $y^\star(t)$ is a *reference* trajectory, and $e(t) = y(t) - y^\star(t)$ is the *tracking* error;
- $K_P, K_D \in \mathbb{R}$ are *tuning* gains.

Eqn. (5) and (6) yield $\ddot{e}(t) + K_D \dot{e}(t) + K_P e(t) = F(t) - F_{\text{est}}(t)$. Select K_P, K_D such that the real parts of the roots of the polynomial $s^2 + K_D s + K_P$ are strictly negative. It ensures that $\lim_{t \to +\infty} e(t) \approx 0$ if the estimate F_{est} is "good" i.e., $F(t) - F_{\text{est}}(t) \approx 0$. Thus local stability around the reference trajectory is trivially ensured via this feedback loop. The following estimate of F in Eqn. (5) is borrowed from [12]:

$$\begin{aligned} F_{\text{est}}(t) = & \frac{60}{\tau^5} \int_0^\tau (\tau^2 + 6\sigma^2 - 6\tau\sigma) y(t - \tau + \sigma) d\sigma \\ & - \frac{30\alpha}{\tau^5} \int_0^\tau (\tau - \sigma)^2 \sigma^2 u(t - \tau + \sigma) d\sigma \end{aligned} \tag{7}$$

- It is a real-time estimate: $\tau > 0$ is "small."
- It is indeed data-driven: the numerical value of F_{est} results from the knowledge of the control and output variables u and y.
- It is a "low pass filter" thanks to the integrals in Formula (7): noise in the sense of [41] are removed.

1) Riachy's trick: It permits [12] to avoid the calculation of the derivative $\dot{e}$ in Eqn. (6). Rewrite (5) as $\ddot{y}(t) + K_D \dot{y}(t) = F(t) + K_D \dot{y}(t) + \alpha u(t)$. Set

$$Y(t) = y(t) + K_D \int_c^t y(\sigma) d\sigma, \quad 0 \leqslant c < t$$

It yields $\ddot{Y}(t) = \ddot{y}(t) + K_D \dot{y}(t)$. Set $\mathscr{F}(t) = F(t) + K_D \dot{y}(t)$. Eqn. (5) becomes $\ddot{Y}(t) = \mathscr{F}(t) + \alpha u(t)$. Eqn. (6) reads now

$$u(t) = -\frac{\mathscr{F}_{\text{est}}(t) - \ddot{y}^\star(t) + K_P e(t) + K_D \dot{y}^\star(t)}{\alpha} \tag{8}$$

where the derivative of y and, therefore, e disappears. The estimate $\mathscr{F}_{\text{est}}$ in Eqn. (8) may be computed via Formula (7) by replacing y by Y.

B. Computer simulations

1) Presentation: The numerical values of the parameters in Eqn. (1) are taken from [36], [37]: $C_1 = 135$, $C_2 = 0.8C_1$, $C_3 = 0.25C_1$, $C_4 = 0.25C_1$, $C_7 = C_2$, $C_5 = 0.3C_1$, $C_6 = 0.1C_1$, $A = 3.25$, $B = 22$, $G = 20$, $a = 100$, $b = 30$, $g = 350$. Following again [36], [37], set

- $p = 200$, $0 \leqslant t \leqslant 2$s, for a regular behavior;
- $p = 800$, $t > 2$s, for an abnormal behavior.

Moreover, p is corrupted by an additive white Gaussian noise (mean: 0, standard deviation: 10).

The stimulation begins when the anomaly is detected. Several scenarios are now presented.

2) Scenarios 1 and 2: Assume that $y_1(t)$ is available. Set $y(t) = y_1(t)$ in Eqn. (5), where $\alpha = 10^4$.[1] Set $K_P = 100$, $K_D = 20$ in Eqn. (6).

In Scenario 1 (Fig. 4) a constant reference is perfectly tracked (Fig. 4-(b)) with very reasonable values of the stimulation: $0 \leqslant u(t) \leqslant 15$ (Fig. 4-(c)). It is quite obvious to check that the very nature of the sigmoid function in Eqn. (1) prevents to track references of arbitrary magnitude. In Scenario 2 (Fig. 5) the reference trajectory is reproducing a crisis-free recording (Fig. 5-(b)). The tracking is again excellent.

3) Scenario 3 – Several virtual patients: Set in Scenario 3 (Figs. 6, 7, 8) $y(t) = y_m(t)$, $\alpha = -10^5$ in Eqn. (5), and $K_P = 400$, $K_D = 40$ in Eqn. (6). The following numerical variations on C_ι, $\iota = 1, \ldots, 7$ correspond to different virtual patients. Take $0.9 \times C_\iota$ (resp. $1.1 \times C_\iota$), $\iota = 1, \ldots, 7$. Results are reported in Fig. 6 (resp. Fig. 7). See Fig. 8 for the results with the nominal values of C_ι. Tracking is excellent in all three cases.

4) Scenario 4 – Measurement noise: Again $y(t) = y_m(t)$, $\alpha = -10^5$ in Eqn. (5), and $K_P = 400$, $K_D = 40$ in Eqn. (8). In Scenario 4 (Fig. 9) an additive white Gaussian noise has been added as a measurement noise (mean: 0, standard deviation: 0.5). Performances deteriorate only slightly with a chattering control variable.

V. Conclusion

Our communication suggests that some recent control techniques, which were already most useful in industry, might also be helpful for implementing closed-loop neurostimulations for curing epileptiform seizures. Even if our results seem, to the best of our knowledge, to surpass the existing literature, there is still a lot of work to be done to go beyond virtual patients. Future publications will soon examine other topics in neuroscience, like Parkinson's disease and brain plasticity.

References

[1] J.W. Antony, H.-V.V. Ngo, T.O., Bergmann, B. Rasch, "Real-time, closed-loop, or open-loop stimulation? Navigating a terminological jungle," *J. Sleep Res.*, 31, 2022, e13755.

[2] S. Martínez, D. García-Violini, M. Belluscio, J. Piriz, R. Sánchez-Peña, "Dynamical models in neuroscience from a closed-loop control perspective," *IEEE Rev. Biomed. Engin.*, 16, 2023, 706-721.

[3] S. Marceglia, M. Guidetti, I.E. Harmsen, A. Loh, S. Meoni, G. Foffani, A.M. Lozano, J. Volkmann, E. Moro, A. "Priori, Deep brain stimulation: is it time to change gears by closing the loop?," *J. Neural Engin.*, 18, 2021, 061001.

[4] J. Rösch, D.E. Vetter, A. Baldassarre, V.H. Souza, P. Lioumis, T. Roine, A. Jooß, D. Baur, G. Kozák, D.B. Jovellar, S. Vaalto, G.L. Romani, R.J. Ilmoniemi, U. Ziemann, "Individualized treatment of motor stroke: A perspective on open-loop, closed-loop and adaptive closed-loop brain state-dependent TMS," *Clinic. Neurophysio.*, 158, 2024, 204-211.

[5] C. Zrenner, U. Ziemann, "Closed-loop brain stimulation," *Biolog. Psych.*, 95, 2024, 545-552.

[1] This numerical value might seem huge to readers which are used to this model-free approach. It is easily explained here by looking at the second line of Eqn. (1) and computing the product AaC_2 in front of the sigmoid function.

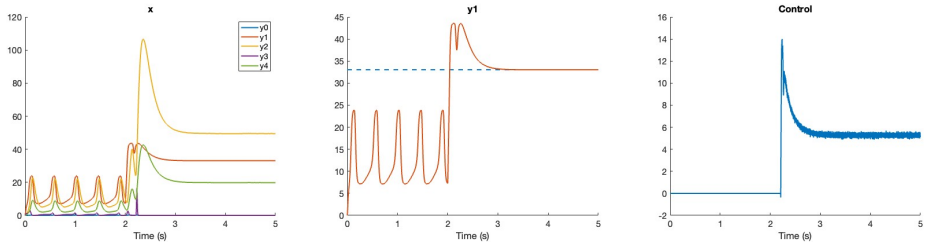

(a) States *(b)* y_1 (red —) and $y^\star$ (blue - -) *(c)* Control input u

Fig. 4. Closed loop result: Scenario 1

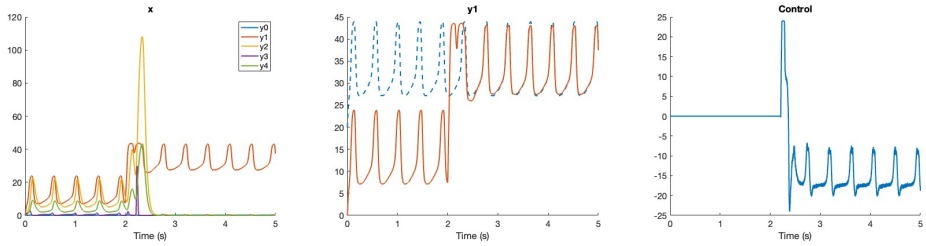

(a) States *(b)* y_1 (red —) and $y^\star$ (blue - -) *(c)* Control input u

Fig. 5. Closed loop result: Scenario 2

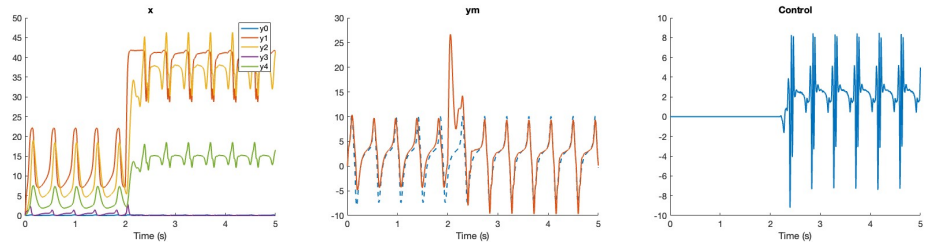

(a) States *(b)* y_m (red —) and $y^\star$ (blue - -) *(c)* Control input u

Fig. 6. Closed loop result: Scenario 3a

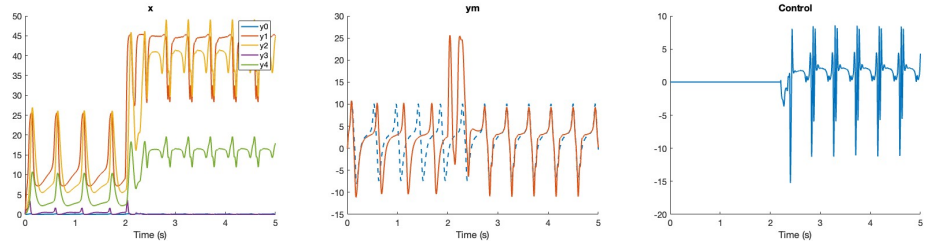

(a) States *(b)* y_m (red —) and $y^\star$ (blue - -) *(c)* Control input u

Fig. 7. Closed loop result: Scenario 3b

[6] H. Kassiri, S. Tonekaboni, M.T. Salam, N. Soltani, K. Abdelhalim, J.L.P. Velazquez, R. Genov, "Closed-loop neurostimulators: A survey and a seizure-predicting design example for intractable epilepsy treatment," *IEEE Trans. Biomed. Circ. Syst.*, 11, 2017, 1026-1040.

[7] E. De Schutter, "Why are computational neuroscience and systems biology so separate?," *Plos Comput. Biol.*, 4, 2008, e1000078.

[8] U. Alon, *An Introduction to Systems Biology* (2nd ed.), CRC Press, 2020.

[9] D. Del Vecchio, R. Murray, *Biomolecular Feedback Systems*, Princeton University Press, 2015.

[10] R.S. Fisher, C. Acevedo, A. Arzimanoglou, A. Bogacz, J.H. Cross, C.E. Elger, J. Engel Jr, L. Forsgren, J.A. French, M. Glynn, D.C. Hesdorffer, B.I. Lee, G.W. Mathern, S.L. Moshé, E. Perucca, I.E. Scheffer, T. Tomson, M. Watanabe, S. Wiebe, "A practical clinical definition of epilepsy," *Epilepsia*, 55, 2014, 475-482.

[11] M. Fliess, C. Join, "Model-free control," *Int. J. Contr.*, 86, 2013, 2228-2252.

[12] M. Fliess, C. Join, "An alternative to proportional-integral and proportional-integral-derivative regulators: Intelligent proportional-derivative regulators," *Int. J. Robust Nonlin. Contr.*, 32, 2022, 9512-9524.

[13] A. Artuñedo, M. Moreno-Gonzalez, J. Villagra, "Lateral control for autonomous vehicles: A comparative evaluation," *Annual Rev. Contr.*, 57, 2024, 100910.

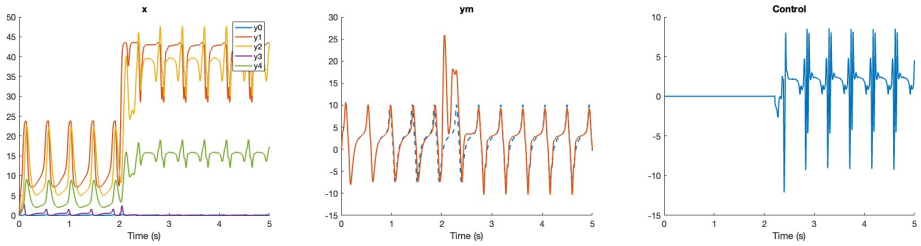

(a) States *(b)* y_m (red —) and $y^\star$ (blue - -) *(c)* Control input u

Fig. 8. Closed loop result: Scenario 3c

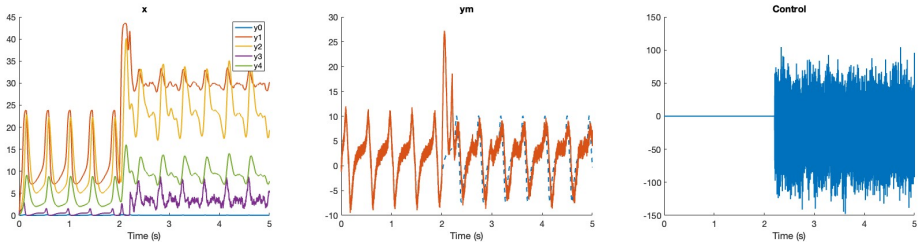

(a) States *(b)* y_m (red —) and $y^\star$ (blue - -) *(c)* Control input u

Fig. 9. Closed loop result: Scenario 4

[14] K.J. Åström, R.M. Murray, *Feedback Systems: An Introduction for Scientists and Engineers* (2nd ed.), Princeton University Press, 2021.

[15] O. Bara, M. Fliess, C. Join, J. Day, S.M. Djouadi, "Toward a model-free feedback control synthesis for treating acute inflammation," *J. Theor. Biol.*, 448, 2018, 26-37.

[16] D. He, H. Wang, Y. Tian, N. Christov, I. Simeonov, "Trajectory tracking of two-stage anaerobic digestion process: A predictive control with guaranteed performance and saturated input, based on ultra-local model," *J. Process Contr.*, 129, 2023, 103039.

[17] E. Manzoni, M. Rampazzo, "Automatic regulation of anesthesia via ultra-local model control," *IFAC PapersOnLine*, 54-15, 2021, 49-54.

[18] T. MohammadRidha, M. Aït-Ahmed, L. Chailloux, M. Krempf, I. Guilhem, J.-Y. Poirier, C.-H. Moog, "Model free iPID control for glycemia regulation of type-1 diabetes," *IEEE Trans. Biomed. Engin.*, 65, 2018, 199-206.

[19] C.T. Truong, K.H. Huynh, V.T. Duong, H.H. Nguyen, L.A. Pham, T.T. Nguyen, "Model-free volume and pressure cycled control of automatic bag valve mask ventilator," *AIMS Bioengin.*, 8, 2021, 192-207.

[20] A. Berényi, M. Belluscio, D. Mao, G. Buzsáki, "Closed-loop control of epilepsy by transcranial electrical stimulation," *Science*, 337, 2012, 735-737.

[21] M.K. Siddiqui, R. Morales-Menendez, X. Huang, N. Hussain, "A review of epileptic seizure detection using machine learning classifiers," *Brain Informat.*, 7, 2020, 5.

[22] L.S Vidyaratne, K.M. Iftekharuddin, "Real-Time epileptic seizure detection using EEG," *IEEE Trans. Neural Syst. Rehabilit. Engin.*, 25, 2017, 2146-2156

[23] G. Wu, K. Yu, H. Zhou, X. Wu, S. Su, "Time-series anomaly detection based on dynamic temporal graph convolutional network for epilepsy diagnosis," *Bioengin.*, 11, 2024, 53.

[24] Q. Yuan, W. Zhou, L. Zhang, F. Zhang, F., Xu, Y. Leng, D. Wei, M. Chen, "Epileptic seizure detection based on imbalanced classification and wavelet packet transform," *Seizure*, 50, 2017, 99-108.

[25] M. Zhou, C. Tian, R. Cao, B. Wang, Y. Niu, T. Hu, H. Guo, J. Xiang, "Epileptic seizure detection based on EEG signals and CNN," *Front. Neuroinformat.*, 12, 2018.

[26] M. Fliess, C. Join, H. Sira-Ramírez, "Non-linear estimation is easy," *Int. J. Model. Identif. Contr.*, 4, 2008, 12-27.

[27] M. Fliess, M. Mboup, H. Mounier, H. Sira-Ramírez, "Questioning some paradigms of signal processing via concrete examples," In G. Silva-Navarro, G., Sira-Ramírez, H. (Eds.): *Algebraic Methods in Flatness, Signal Processing and State Estimation* (Chapter 1), Innovación Editorial Lagares De México, 2003.

[28] M. Fliess, H. Sira-Ramírez, "An algebraic framework for linear identification," *ESAIM COCV*, 9, 2003, 151-168.

[29] M. Fliess, C. Join, "Fouille de données et segmentation de chroniques par extrema: considérations préliminaires," *13^e Conf. Francoph. Modélis. Optim. Simu. (MOSIM'20)*, Agadir, 2020. arxiv:2009.09895

[30] M. Mboup, C. Join, M. Fliess, "Numerical differentiation with annihilators in noisy environment," *Numer. Algo.*, 50, 2009, 439-467.

[31] A. Othmane, L. Kiltz, J. Rudolph, "Survey on algebraic numerical differentiation: historical developments, parametrization, examples, and applications," *Int. J. Syst. Sci.*, 53, 2022, 1848-1887.

[32] F. Wendling, F. Bartolomei, J.J. Bellanger, P. Chauvet, "Epileptic fast activity can be explained by a model of impaired GABAergic dendritic inhibition," *Eur. J. Neurosci.*, 15, 2002, 1499-1508.

[33] B.H. Jansen, V.G. Rit, "Electroencephalogram and visual evoked potential generation in a mathematical model of coupled cortical columns," *Bio. Cybern.*, 73, 1995, 357-366.

[34] L.A. Ferrat, M. Goodfellow, J.R. Terry, "Classifying dynamic transitions in high dimensional neural mass models: A random forest approach," *PLoS Comput. Biol.*, 14, 2018, e1006009.

[35] F. Wendling, P. Benquet, F. Bartolomei, V. Jirsa, "Computational models of epileptiform activity," *J. Neurosci. Meth.*, 260, 2016, 233-251.

[36] M. Arrais, *Stimulation cérébrale multisites: Modèles dynamiques et application aux crises d'épilepsie* (in English). Thèse, Université de Rennes, 2020.

[37] M. Arrais, F. Wendling, J. Modolo, "Identification of effective stimulation parameter to abort seizures in a neural mass model," *41st Int. Conf. IEEE Engin. Med. Biol. Soc.*, Berlin, 2019, pp. 5208-5211.

[38] M. Arrais, J. Madolo, D. Mogul, F. Wendling, "Design of optimal multi-site brain brain stimulation protocols via neuro-inspired epilepsy models for abatement of interictal discharges," *J. Neural Engin.*, 18, 2021, 016024.

[39] T. Radman, R.L. Ramos, J.C. Brumberg, M. Bikson, "Role of cortical cell type and morphology in subthreshold and suprathreshold uniform electric field stimulation in vitro," *Brain Stimu.*, 2, 2009, 215-228.

[40] K. Yosida, *Operational Calculus* (translated from the Japanese), Springer, 1984.

[41] M. Fliess, "Analyse non standard du bruit," *C.R. Math.*, 342, 2006, 797-802.

[42] C.E. Cook, M. Bernfeld, *Radar Signals*, Artech House, 1993.